Molecular Crystals and Liquid Crystals

Publication details, including instructions for authors and subscription information:
http://www.tandfonline.com/loi/gmcl20

Thermodynamical and Optical Studies of Ternary Mixtures of 4-n-Heptyloxy Benzoic Acid, 4-n-Decyloxy Benzoic Acid, and 5-Cholesten-3ß-ol 3-octanoate

R. Dhar [a] , M. B. Pandey [a] & V. K. Agrawal [b]

[a] Physics Department, Ewing Christian College, Allahabad, (India)

[b] Physics Department, Allahabad University, Allahabad, (India)

Version of record first published: 18 Oct 2010

To cite this article: R. Dhar, M. B. Pandey & V. K. Agrawal (2004): Thermodynamical and Optical Studies of Ternary Mixtures of 4-n-Heptyloxy Benzoic Acid, 4-n-Decyloxy Benzoic Acid, and 5-Cholesten-3ß-ol 3-octanoate, Molecular Crystals and Liquid Crystals, 409:1, 269-284

To link to this article: http://dx.doi.org/10.1080/15421400490431408

Mol. Cryst. Liq. Cryst., Vol. 409, pp. 269–284, 2004

ISSN: 1542-1406 print/1563-5287 online
DOI: 10.1080/15421400490431408

THERMODYNAMICAL AND OPTICAL STUDIES OF TERNARY MIXTURES OF 4-n-HEPTYLOXY BENZOIC ACID, 4-n-DECYLOXY BENZOIC ACID, AND 5-CHOLESTEN-3β-OL 3-OCTANOATE

R. Dhar and M. B. Pandey
Physics Department, Ewing Christian College, Allahabad-211 003 (India)

V. K. Agrawal
Physics Department, Allahabad University, Allahabad-211 002 (India)

Binary eutectic mixture of 4-n-heptyloxybenzoic acid (HOBA) and 4-n-decyloxybenzoic acid (DOBA) shows smectic C (SmC) and nematic (N) phases over a wide temperature range. 5-cholesten-3β-ol 3-octanoate(ChO), which has monotropic chiral nematic (N^*) phase, has been added as third component in the eutectic bi-component mixture (BCM) of HOBA-DOBA in different mole ratios. Transition temperatures and enthalpies of the ternary mixtures have been determined by using differential scanning calorimeter (DSC) and mesophases have been identified with the help of polarizing microscope. It has been observed that the thermal stability of SmC phase of BCM decreases rapidly due to the addition of ChO molecules and SmC phase is completely suppressed for about 10–12 mole percent of ChO. A narrow temperature range TGBC phase has been observed for ChO concentrations 2 to 8 mole percent. For higher concentrations of ChO molecules, TGBA and SmA phases have been induced over a wide temperature range. Ternary system of ChO and BCM shows N^* phase over a wide temperature range in the heating and cooling cycles at about eutectic composition (12.5 mole percent of ChO) of ChO-BCM system.

Keywords: 4-n-decyloxybenzoic acid; eutectic mixture; ternary mixture; TGB phase

We thank University Grants Commission (UGC), New Delhi-110 002 for financial assistance under a major research project No.F.10-81/2001. One of us (MBP) thanks to UGC for a research fellowship under the project. We express our sincere thanks to Prof. S. L. Srivastava, Coordinator, K. Banerjee Centre for Atmospheric and Ocean Studies, Allahabad University, Allahabad for his valuable comments on the present work.

Address correspondence to R. Dhar, Physics Department, Ewing Christian College, Allahabad-211 003 (India). E-mail: dr_ravindra_dhar@hotmail.com

INTRODUCTION

Binary mixtures of cholesteric and nematic liquid crystals show many interesting molecular interactions resulting in different kinds of frustrated/induced mesophases including recently observed twist grain boundary (TGB) phases of Renn and Lubenski [1–3]. First binary mixture which shows the TGBA phase was the mixture of 5-cholesten-3β-ol 3-nonanoate (ChN) and 4-n-nonyloxybenzoic acid (NOBA) [4]. We have done extensive thermodynamical, optical and electrical studies on this mixture [5]. Since then many other nematic-cholesteric mixtures have been found to show a large variety of TGB phases. Re-entrant phenomenon of TGB phases has also been reported in the binary mixtures [6]. The mixtures of cholesteryl esters with nematics are expected to show TGB phases because of the twisting power of cholesterol [7]. We have reported TGBA phase in the binary mixtures of 5-cholesten-3β-ol 3-tetradecanoate with 4-n-dodecyloxybenzoic acid also [8]. Experimental data (specially calorimetric) on TGB phases are still very scarce and so more and more systems are needed to be checked for experimental data as well as to explore new TGB phases [9]. It is interesting to note that few workers have explored tri component mixtures and observed TGBA and TGBC phases [10].

In the present paper we are reporting the optical and thermodynamical results on the tri component mixtures. Tri component mixtures have been prepared by adding different mole percents of 5-cholesten-3β-ol 3-octanoate (ChO) in the eutectic bi component mixture of 4-n-heptyloxybenzoic acid (HOBA) and 4-n-decyloxybenzoic acid (DOBA). SmC and N mesophases of 4-n-alkyloxybenzoic acid series are lowered for the eutectic binary mixture of 4-n-heptyloxybenzoic acid and 4-n-decyloxybenzoic acid [11]. The eutectic bi component mixture (BCM) of 4-n-heptyloxybenzoic acid and 4-n-decyloxybenzoic acid has been found to be 53:47 (mole percent ratio) with the phase sequence K←(60.0/°C)→SmC←(104.3)→N←(142.2)→I. Molecular length of ChO is shorter by one alkyl chain in comparison to ChN but it has only monotropic N^* mesophase unlike SmA and N^* phases in ChN and 5-cholesten-3β-ol 3-tetradecanoate. Therefore it is interesting to see the mixtures of ChO and BCM. Phase sequence of ChO is as follows:

$$\text{K}\text{–}(106.8/^\circ\text{C}) \rightarrow \text{I} - (92.2) \rightarrow \text{N}^* - (71.6) \rightarrow \text{K}.$$

EXPERIMENTAL TECHNIQUES

Pure samples of 5-cholesten-3β-ol 3-octanoate (ChO), 4-n-heptyloxybenzoic acid (HOBA) and 4-n-decyloxybenzoic acid (DOBA) have been procured from Institute of Physics, Academy of Sciences of Ukraine, Kiev

(Ukraine). Sixteen ternary mixtures of different mole ratios of ChO with eutectic mixture of HOBA and DOBA (BCM) have been prepared. For weighing the samples, an electro balance of Cahn (model C-33) having an accuracy of 1 μg has been used. Before taking the measurements, these mixtures have been homogenized by adequate stirring in their isotropic liquid phase.

Different mesophases of the mixtures have been identified with the help of polarizing microscope. Temperature of the samples kept between two cover slips of glass under the microscope has been controlled with the help of a hot stage of Instec with temperature accuracy of ± 3 mK. Different mesophase transition temperatures (T_P) and transition enthalpies (ΔH) have been determined by using a Differential Scanning Calorimeter of Perkin-Elmer (model DSC-7) at the scanning rate of 10 K-min^{-1}. DSC has been calibrated using zinc and indium at the scanning rate of 10 K-min^{-1}. Peak transition temperatures (T_P) have been determined with the accuracy of ± 0.1 K whereas transition enthalpies (ΔH) have been determined with the accuracy better than 5% for fully-grown peaks. However for very weak peaks uncertainties are large.

RESULTS AND DISCUSSION

Phase diagrams (T_P vs. mole percent of BCM in ChO) for the heating and cooling cycles have been drawn using peak transition temperatures (T_P) obtained from DSC and are shown in Figures 1 and 2 respectively. Phase diagram of ChO-BCM system in the heating cycle shows usual eutectic phase diagram of binary systems with the eutectic composition at 12.5 mole percent of ChO (87.5 mole percent of BCM) and eutectic temperature (T_e) at 58.0°C. Monotropic N* phase of pure ChO appears in the heating cycle also for BCM concentration above 30 mole percent (see Fig. 1). Range of N* phase increases with BCM concentration. Range of SmC phase of BCM decreases with the addition of ChO and is completely suppressed at about 10 mole percent of ChO in BCM leaving wide range N* phase at eutectic composition. Figure 1 thus shows that behaviour of eutectic BCM is similar as if a single system has been mixed with ChO.

Calculations for Eutectic Composition

Eutectic composition of ChO-BCM system has also been estimated by empirical relationship [12]

$$x_e = \frac{(T_2 - T_e)}{T_1 + T_2 - 2T_e} \tag{1}$$

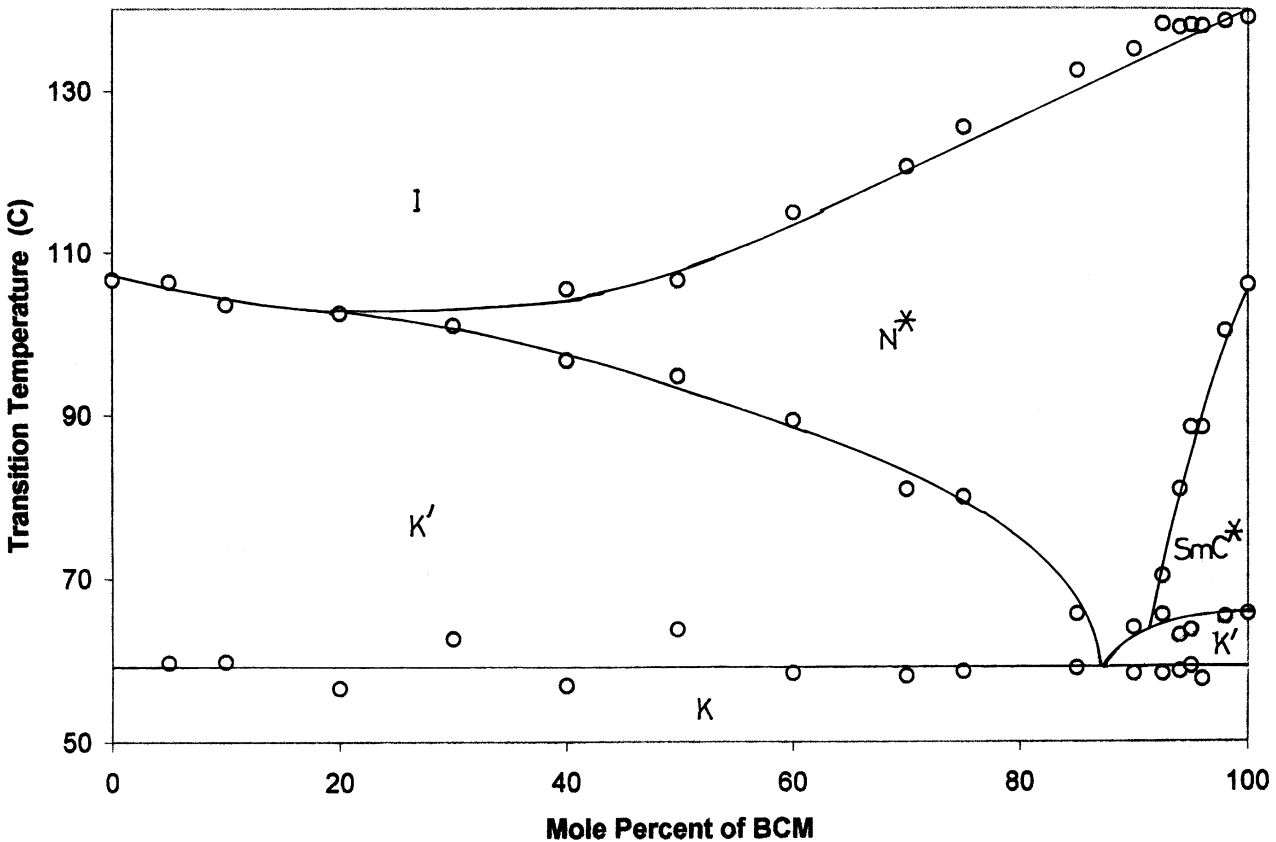

FIGURE 1 Phase diagram (transition temperature/°C with mole percent of BCM) for the ChO-BCM system in the heating cycle. K′ is the mixed crystal phase.

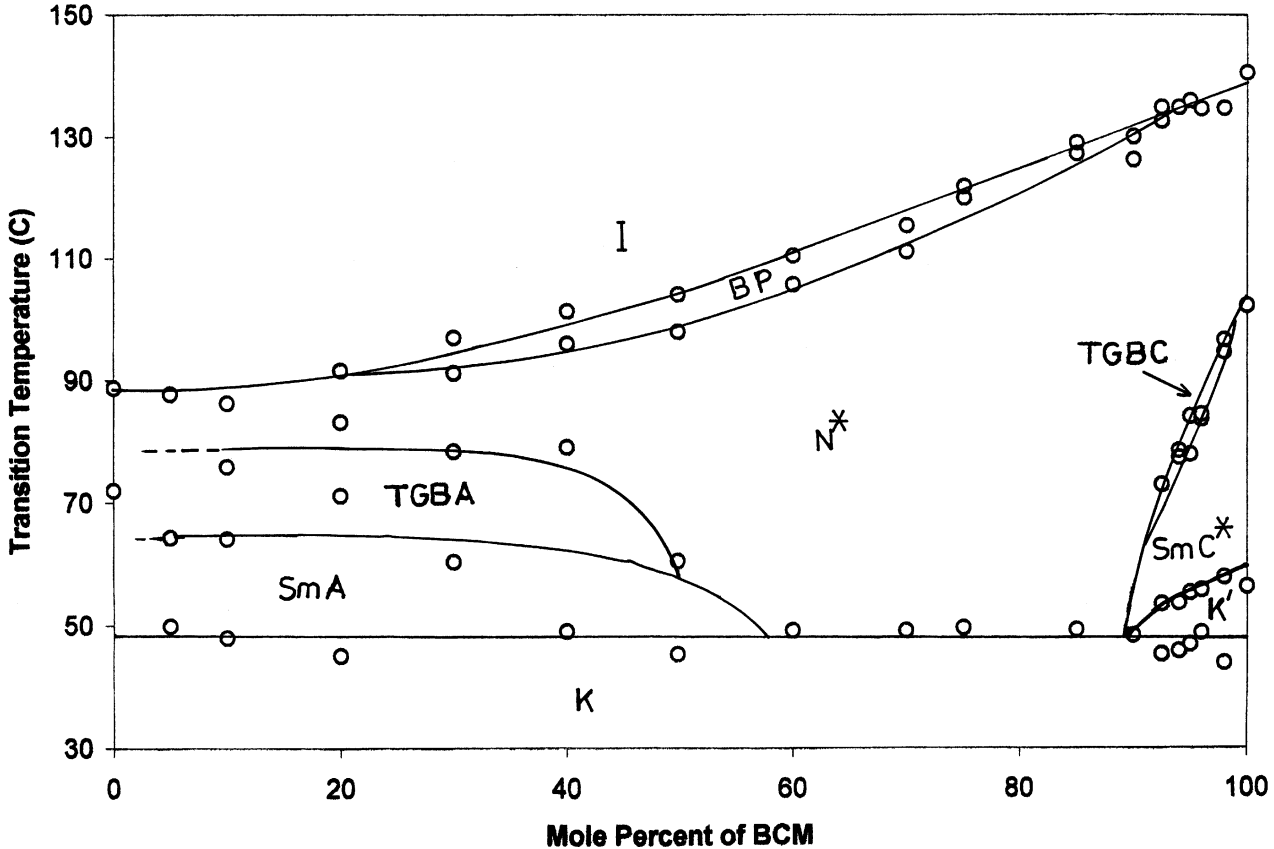

FIGURE 2 Phase diagram (transition temperature/°C with mole percent of BCM) for the ChO-BCM system in the cooling cycle.

where T_1 and T_2 are melting points of BCM and ChO, T_e is eutectic temperature and x_e is the eutectic mole fraction of lower melting component (BCM). Taking $T_1 = 338.9\,K$ and $T_2 = 379.9\,K$, Eq. (1) gives eutectic composition at 86.3 mole percent of BCM which is very close to the value observed by the phase diagram (87.5 mole percent).

Schroder-Van Laar equation [13,14] has also been applied on BCM to find the eutectic composition of ChO-BCM system

$$\ln x_e = \frac{\Delta H_{1K}}{R}\left(\frac{1}{T_1} - \frac{1}{T_e}\right) - \ln f_i \tag{2}$$

where ΔH_{1K} is the crystal to mesophase transition enthalpy of BCM. f_i is the activity coefficient and is 1 for ideal mixed phases [13]. Taking $\Delta H_{1K} = 15.3\,kJ\text{-}mol^{-1}$, $R = 8.318\,J\text{-}mol^{-1}\text{-}K^{-1}$) and $f_i = 1$, value of eutectic composition has been found to be 88.2 mole percent of BCM which is almost same as obtained from phase diagram in Eq. (1). This shows the validity of Schroder-Van Laar equation [13] for multi component systems as well. If Schroder-Van Laar equation [13,14] is applied on ChO as

$$\ln(1 - x_e) = \frac{\Delta H_{2K}}{R}\left(\frac{1}{T_2} - \frac{1}{T_e}\right) - \ln f_i \tag{3}$$

then value of eutectic composition comes out to be 77.8 mole percent of BCM (with $f_i = 1$) that is slightly away from actual value (87.5 mole percent) from Figure 1. In Eq. (3) $\Delta H_{2K} = 32.3\,kJ\text{-}mol^{-1}$ is the crystal to mesophase transition enthalpy of ChO. Results from Eqs. (2) and (3) show that Schroder-Van Laar equation is better applicable on the component of the system toward which eutectic point lies. For eutectic composition at 87.5 mole percent of BCM, the value of $\ln f_i$ in Eq. (3) comes out to be 0.575 which gives the excess free energy of the system at the eutectic composition $(G_e^E) = 0.5\,kJ/mol$ where

$$G_e^E = \frac{RT_e \ln f_i}{4(1 - x_e)^2} \tag{4}$$

The value of excess free energy G_e^E is only 1.5% of ΔH_{2K}. However actual deviation in total enthalpy at eutectic composition is far more than this value (see Fig. 3).

Figure 3 shows the variation of total melt enthalpy and entropy with mole percent of BCM. Crystal (K) to mixed phase (K′) transition enthalpy ($\Delta H_{K\text{-}K'}$) increases with the concentration of BCM and reaches a maximum at about eutectic composition. Mixed phase to meso/isotropic transition enthalpy ($\Delta H_{K'\text{-}meso}$) decreases with the concentration of BCM and shows a minimum at about eutectic composition. Thereafter $\Delta H_{K'\text{-}Meso}$ increases with concentration of BCM and reaches maximum for 100 mole percent

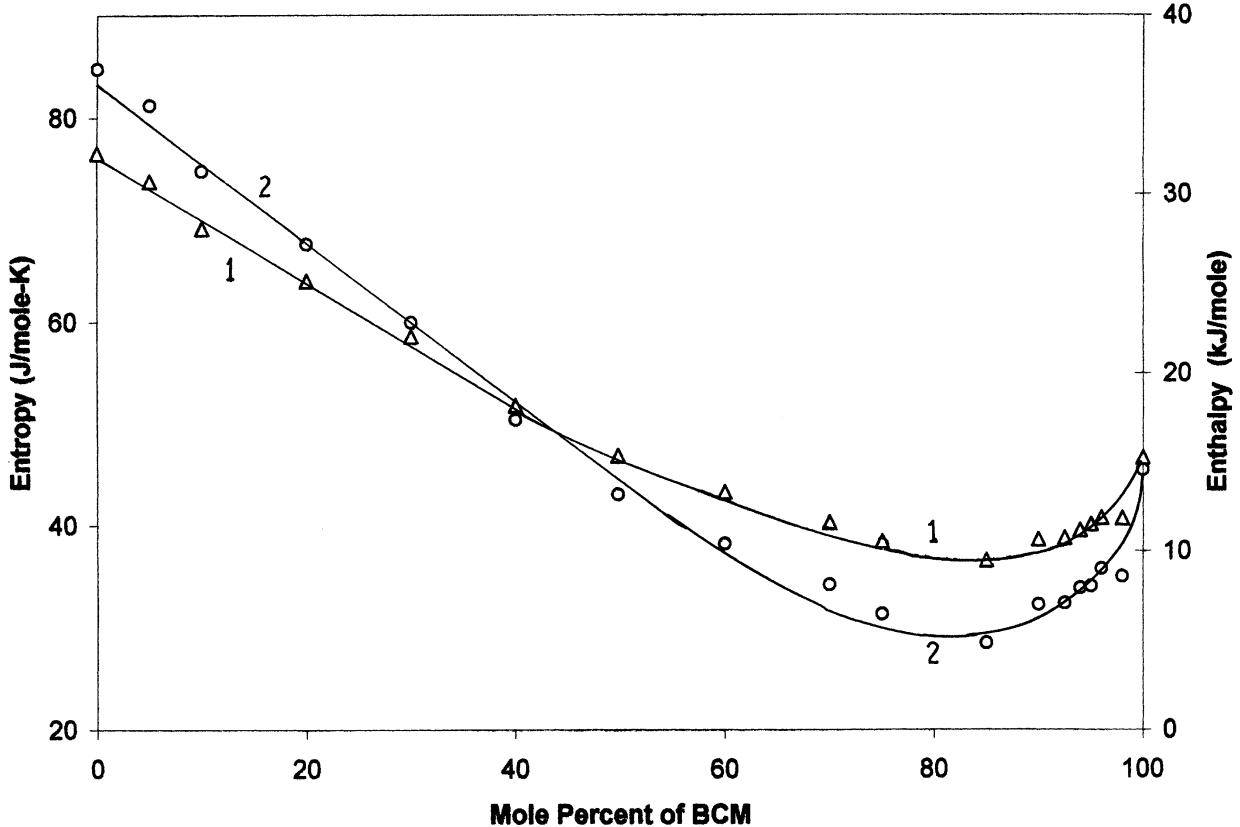

FIGURE 3 Variation of total melting enthalpy (curve 1) and entropy (curve 2) with mole percent of BCM in the heating cycle.

of BCM. It has not been possible to determine $\Delta H_{K\text{-}K'}$ in the range of 90 to 100 mole percent of BCM due to limitation of analysis. Sum of the two enthalpies $\Delta H_{K\text{-}K'}$ and $\Delta H_{K'\text{-meso}}$ is shown in Figure 3 and it deviates from an ideal mixing rule of enthalpy. Deviation is largest at the eutectic composition where it shows minimum as observed in most of the other mixtures. Similar features have been obtained for the entropies for these transitions. Minima of total enthalpy and entropy for eutectic composition shows that eutectic composition is the most stable system.

TGB Phases

Phase diagram for the cooling cycle of ChO-BCM system is more interesting than that of the heating cycle. Figure 2 shows that SmA and TGBA phases are induced as soon as BCM is added in ChO. A typical optical texture of TGBA phase in unaligned sample is shown in Figure 4 that resembles the optical textures observed by the other workers [15–17]. We have also observed typical homeotropic textures of TGBA phase [18–20] as shown in Figure 5. However, alignment of the sample does not seem to be perfect homeotropic due to non-uniform thickness of the sample kept between two cover slips coated with the lecithin. Temperature ranges of both TGBA and SmA mesophases have been found to be almost constant up to about 40 mole percent of BCM and thereafter decreases (see Fig. 2). Cooling phase diagram suggests that TGBA phase exists up to about 50 mole percent of

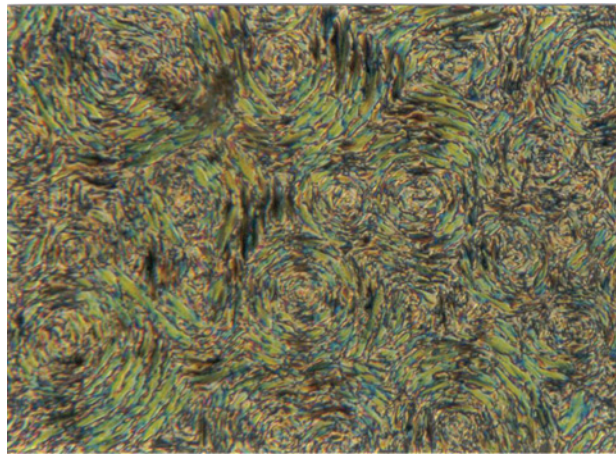

FIGURE 4 Optical texture of TGBA phase in the cooling cycle of mixture with 30 mole percent of BCM (unaligned sample) with magnification 100X. (See COLOR PLATE X)

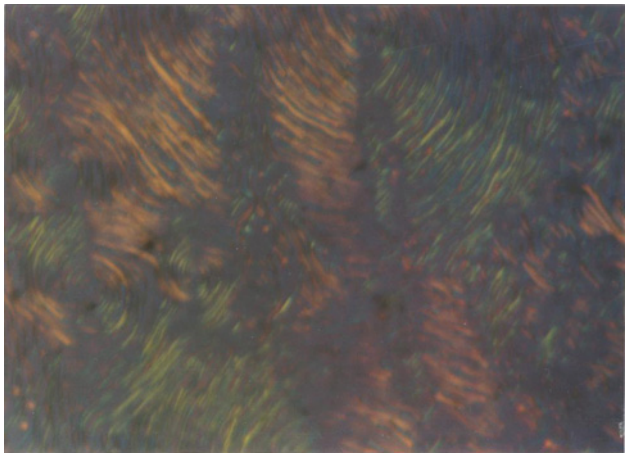

FIGURE 5 Optical texture of TGBA phase in the cooling cycle of mixture with 20 mole percent of BCM (homeotropic aligned sample) with magnification 100X. (See COLOR PLATE XI)

BCM whereas SmA phase exists up to 60 mole percent of BCM. In the cooling cycle also, range of SmC phase of BCM decreases very quickly with the increasing concentration of ChO as observed in the heating cycle (see Figs. 1 and 2). TGBC phase has also been observed in small range of BCM concentrations lying between 93 to 98 mole percent. Albeit the temperature range of the thermodynamically stable TGBC phase is very small as shown in Figure 2. Optical textures of TGBC and SmC* phases are similar to those obtained in ChO-NOBA system [21]. For unaligned samples, optical texture of TGBC phase is almost similar to TGBA phase as predicted and observed by others [9,10] but the spiral fans are thin in comparison to those in TGBA. Phase diagram clearly separates the TGBA and TGBC phases by wide range cholesteric gap in Figure 2.

Transition temperatures, transition enthalpies and transition entropies related with the various transitions involving TGB phases are given in Table 1. Several other workers have observed the transition enthalpies and entropies related with the transitions involving TGBA phase of the same order [22–25]. It has not been possible to calculate the transition enthalpies and hence entropies separately for N* to TGBC transitions in ChO-BCM system. Table 1 shows that transition temperature, transition enthalpy and transition entropy for N* to TGBA transition are the highest for the mixture having BCM concentration 20 mole percent showing maximum stability of TGBA phase in this mixture. Beyond 20 mole percent of BCM, stability of TGBA phase seems to decrease gradually and finally disappears at about 50 mole percent of BCM (see Fig. 2). While working with

TABLE 1 Transition Temperatures (T_P/°C), Transition Enthalpies (ΔH/J-mol^{-1}) and Transition Entropies (ΔS/J-mol^{-1}-K^{-1}) for N*-TGBA, TGBA-SmA, N*-TGBC and TGBC-SmC* Transitions

Mixtures	N*-TGBA			TGBA-SmA			N*-TGBC			TGBC-SmC*		
ChO: BCM	T_P	ΔH	ΔS	T_P	ΔH	ΔS	T_P	ΔH	ΔS	T_P	$\Delta H^{\clubsuit}$	$\Delta S^{\clubsuit}$
90:10	75.9	40.5	0.116	64.1	23.37	0.069						
80:20	83.2	82.1	0.230	71.1	60.25	0.175						
70:30	78.4	43.4	0.124	60.4	200.75	0.602						
60:40	79.1	38.9	0.110	–	–	–						
06:94							78.6	–	–	77.4	316	0.902
05:95							84.6	–	–	78.0	490	1.396
04:96							84.5	–	–	83.7	488	1.367
02:98							96.7	–	–	94.7	897	2.438

$^{\clubsuit}$Shows total enthalpy and entropy for N*-SmC* as it has not been possible to calculate these quantities separately for N*-TGBC and TGBC-SmC* transitions.

the polarizing microscope, ranges of TGBA and SmA phases have been found to be smaller than shown in Figure 2, which has been drawn by using DSC data. We have observed that under the polarizing microscope, most of the times mixtures crystallize directly from N* phase without going to TGBA and SmA phase. This happens perhaps due to formation of nucleation centres in the samples kept open between two slides. However

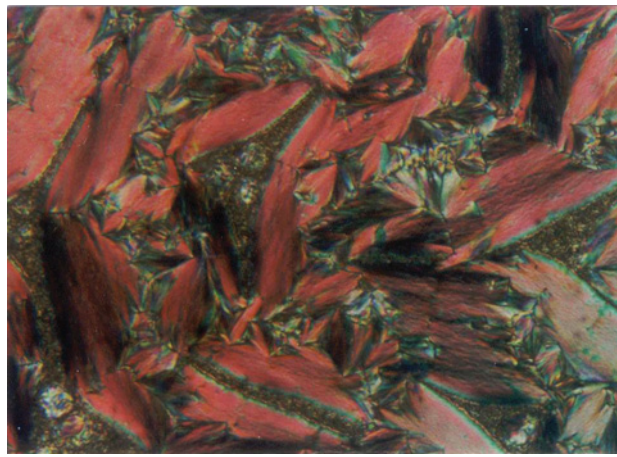

FIGURE 6 Optical fan shape texture of N* phase in the cooling cycle of mixture with 94 mole percent of BCM (unaligned sample) at with magnification 100X. (See COLOR PLATE XII)

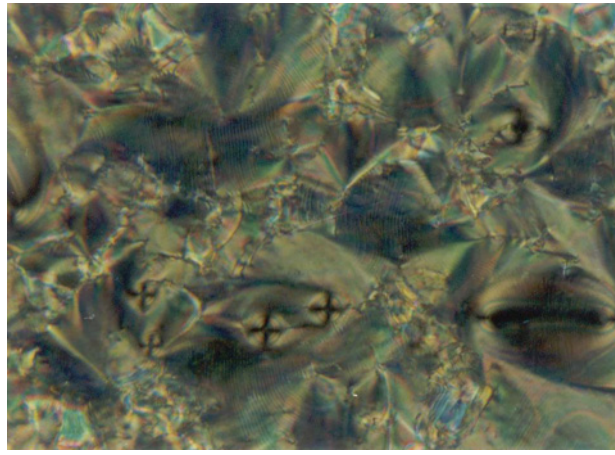

FIGURE 7 Optical fingerprint texture of N* phase in the cooling cycle of mixture with 98 mole percent of BCM (unaligned sample) with magnification 100X. (See COLOR PLATE XIII)

it does not happen in the mixtures where TGBC and SmC* phases exist. A wide temperature range N* phase lying between BCM concentrations 58 and 88 mole percent separates the SmA and SmC phases. The optical texture of N* phase is moss and net like in the concentration range of 0 to 88 mole percent of BCM. Optical texture of N* phase is fan shape in the mixtures where SmC* phase exist giving an impression for SmA phase (see Fig. 6). For the mixture with 98 mole percent of BCM we have observed stripped fan shape texture reminiscent of SmA* phases in ferroelectric liquid crystals (FLCs). To remove the doubts we have checked textures of planar and homeotropic aligned samples and also carried dielectric studies. With the planar alignment we get polygonal domain texture whereas with the homeotropic alignment we get fingerprint textures (Fig. 7) of cholesteric phases [26]. Phase diagram of Figure 2 also suggests it to be N* phase. More so dielectric studies of these mixtures do not show ferroelectric properties. Blue phase has also been observed between the BCM concentrations 20 and 90 mole percent. This also ensures the observed phase to be cholesteric.

I-N* Transition Enthalpy

Enthalpy (ΔH) and entropy (ΔS) of I-N* transitions are governed by the following mixing rules [5].

$$\Delta H = x_1\Delta H_1 + x_2\Delta H_2 + A_H(x_1\Delta H_1 x_2\Delta H_2)^{1/2} \quad (5)$$

$$\Delta S = x_1\Delta S_1 + x_2\Delta S_2 + A_S(x_1\Delta S_1 x_2\Delta S_2)^{1/2} \quad (6)$$

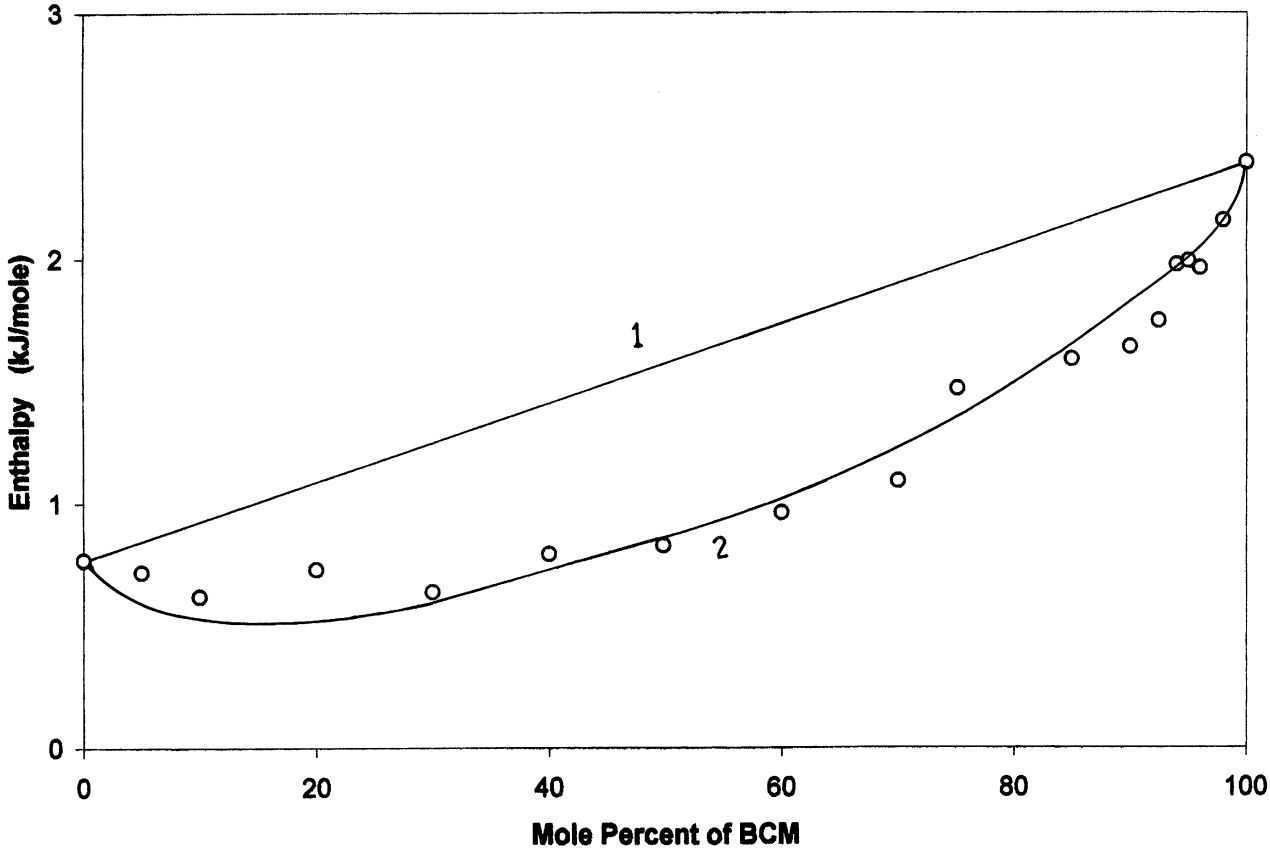

FIGURE 8 Variation I-N* transition enthalpy with mole percent of BCM in the cooling cycle. Curve 1 for ideal mixing with $A_H = 0$ and curve 2 for $A_H = -1.06$ in Eq. (5).

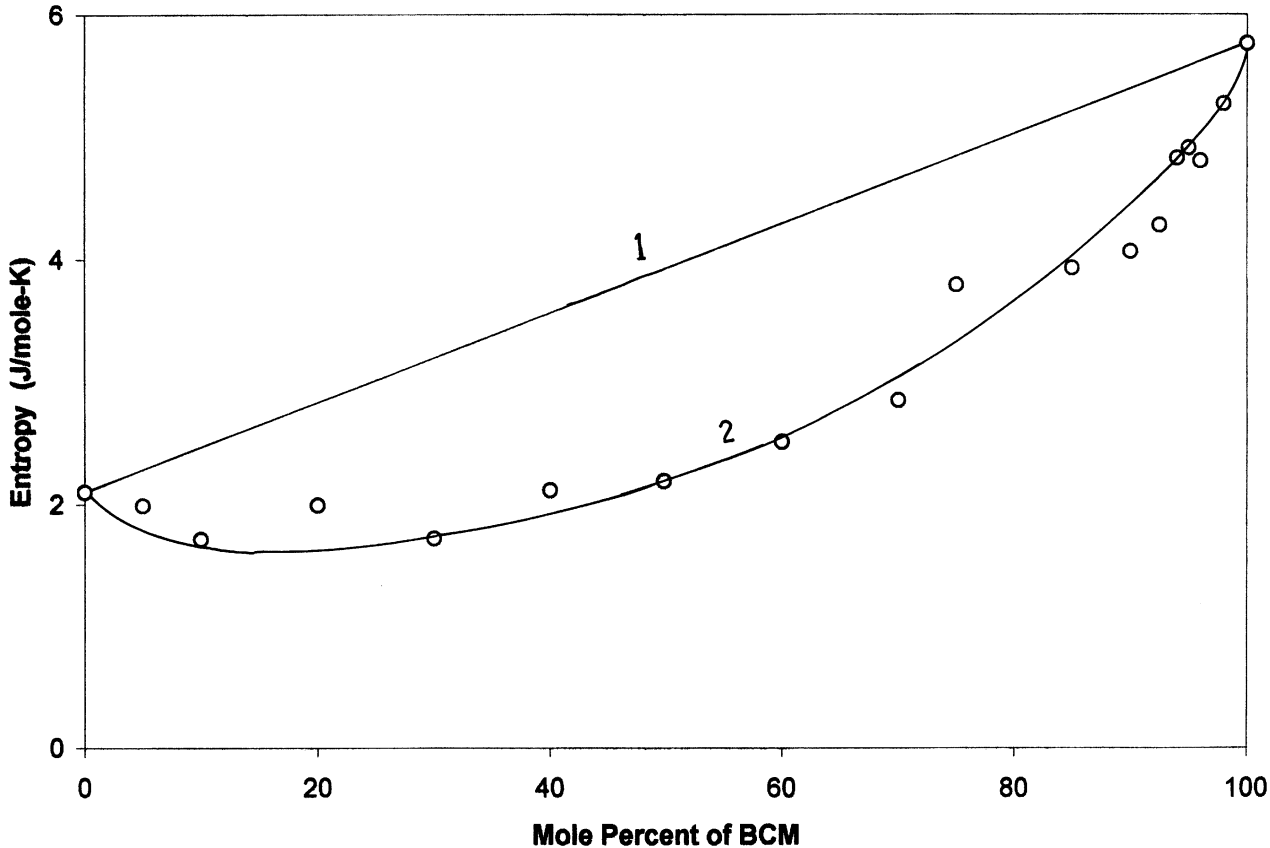

FIGURE 9 Variation I-N* transition entropy with mole percent of BCM in the cooling cycle. Curve 1 for ideal mixing with $A_S = 0$ and curve 2 for $A_S = -0.93$ in Eq. (6).

where x_1, ΔH_1, ΔS_1 are mole fraction, enthalpy and entropy for BCM and x_2, ΔH_2, ΔS_2 are the respective parameters for ChO. The best fit values of the mixing constants A_H and A_S for I to N^* transition have been found to be $-(1.06 \pm 0.21)$ and $-(0.93 \pm 0.19)$ respectively. Plots of ΔH and ΔS for I-N^* transitions are given in Figures 8 and 9 with the best fit values of A_H and A_S for the experimental data. Straight line plots for ΔH and ΔS in Figures 8 and 9 are with A_H and $A_S = 0$ (for hypothetical non interacting ideal mixtures). Negative values of A_H and A_S for I-N^* transition suggest that mixing terms of Eqs. (5) and (6) are destabilizing N^* phase in the mixture. We have already suggested that in BCM, there are molecules of different length due to the formation of monomers and dimers of different length and therefore presence of these monomers and dimers cause disorder in the system [11]. Presence of ChO molecules in ChO-BCM system further increases the randomness and hence causes strong deviation of I-N^* enthalpy and entropy of the system. This also accounts for the non-linearity with negative deviation in the plot of $T_{I\text{-}N^*}$ in Figures 1 and 2.

Comments on the Packing

We have proposed a packing model in the binary mixtures of ChN and NOBA where ChN molecules are stacked between the two dimers of NOBA molecules [5]. However in BCM, five different type of molecular clusters viz. monomers of HOBA and DOBA molecules, dimers of two HOBA molecules, dimers of two DOBA molecules and dimers of HOBA and DOBA molecules are expected. Numbers of monomers are expected to be the largest in the isotropic liquid phase. With the decrease of temperature, numbers of monomers are expected to decrease whereas numbers of dimers are expected to increase. In SmC phase of BCM most of the HOBA and DOBA molecules are expected to be in the form of the dimers [5,27] but when ChO molecules come between these dimers, dipolar forces responsible for tilted layered phase decrease [5]. Hence stability of SmC phase decreases with the increase in the concentration of ChO molecules. ChO molecule is shorter than ChN molecule just by one alkyl chain and this difference causes absence of SmA phase in ChO (whereas SmA phase is present in ChN). Presence of the dimers in the matrix of ChO molecules increases effective molecular length and hence induces layered SmA phase again. The competition between molecules to form cholesteric like structure (due to twisting power of ChO) as well as layered SmA phases may result in frustrated TGBA structure. However with the decrease in ChO concentration (increase in the BCM) first twisting of the SmA blocks diminishes and hence TGBA phase suppresses (see Fig. 2). Further increase in the BCM concentration destroys even the layering due to the competition between ChO molecules to form SmA phase (ChO has hidden

SmA) and dimers to form SmC phase. Twisting power of the ChO is also responsible for TGBC phase. This is a crude molecular packing arrangement based on the bulk properties and the exact molecular packing can be suggested only after some other spectroscopic experiments are carried out.

CONCLUSIONS

Ternary system of ChO (5-cholesten-3β-ol 3-octanoate) with BCM (eutectic composition of 4-n-heptyloxybenzoic acid and 4-n-decyloxybenzoic acid) shows simple eutectic phase diagram like those of binary systems. Low concentrations of ChO molecules (up to about 8 mole percent) in BCM twist the SmC blocks to form TGBC phase. Similarly addition of BCM in ChO induces TGBA and SmA phases in the cooling cycle. A wide range cholesteric gap separates the two TGB phases. The ChO-BCM system shows strong deviation from ideal mixing of enthalpies and entropies.

REFERENCES

[1] Lisetski, L. N., Batrachenko, L. A., & Panikarskaya, V. D. (1992). *Mol. Cryst. Liq. Cryst.*, *215*, 287.
[2] Renn, S. R. & Lubenski, T. C. (1988). *Phys. Rev. A*, *38*, 2132; Booth, C. J., Goodby, J. W., Toyne, K. J., Dunmur, D. A., & Kang, J. S. (1995). *Mol. Cryst. Liq. Cryst.*, *260*, 39.
[3] Kitzerow, H. S. (2001). *Twist grain boundary phases in chirality in liquid crystals*, Kitzerow, H. S. & Bahr, C. (Eds.), Springer-Verlag: New York, 296.
[4] Lavrentovich, O. D., Nastishin, Y. A., Kulishov, V. I., Narkevich, Y. S., & Tolochko, A. S. (1990). *Europhys. Lett.*, *13*, 313.
[5] Srivastava, S. L., Dhar, R., & Mukherjee, A. (1996). *Mol. Crys. Liq. Cryst.*, *287*, 139; Srivastava, S. L. & Dhar, R. (1998). *Mol. Cryst. Liq. Cryst.*, *317*, 23.
[6] Vill, V., Tunger, H. W., & Peters, D. (1996). *Liq. Cryst.*, *20*, 547.
[7] Kuczynski, W. & Stegemeyer, H. (1995). *Mol. Cryst. Liq. Cryst.*, *260*, 377. Kuczynski, W. (1997). *Self Organization in Chiral Liquid Crystals*, Scientific Publishers OWN: Poznan.
[8] Srivastava, S. L. & Dhar, R. (2001). *Mol. Cryst. Liq. Cryst.*, *366*, 79.
[9] Renn, S. R. (1992). *Phys. Rev. A*, *45*, 953; Brunet, M., Navailles, L., & Clark, N. A. (2002). *Euro. Phys. J E*, *7*, 5.
[10] Kramarenko, N. L., Kulishov, V. I., Kutulya, L. A., Semenkova, G. P., Seminozhenko, V. P., & Shkolnikova, N. I. (1997). *Liq. Cryst.*, *22*, 535.
[11] Dhar, R., Pandey, R. S., & Agrawal, V. K. (2002). *Ind. J. Pure Appl. Phys.*, *40*, 901.
[12] Hsu, E. C. H. & Johnson, J. F. (1974). *Mol. Cryst. Liq. Cryst.*, *27*, 95.
[13] Demus, D., Fietkau, C., Schubert, R., & Kehlen, H. (1974). *Mol. Cryst. Liq. Cryst.*, *25*, 215.
[14] Ivashchenko, A. V., Titov, V. V., & Kovshev, E. I. (1976). *Mol. Cryst. Liq. Cryst.*, *33*, 195.
[15] Narihiro, H., Dai, X., Goto, H., & Akagi, K. (2001). *Mol. Cryst. Liq. Cryst.*, *365*, 363.
[16] Malthete, J., Jacques, J., Tinh, N. H., & Destrade, C. (1982). *Nature*, *298*, 46.
[17] Chen, J. H., Chang, R. C., Hsiue, G. H., Guu, F. W., & Wu, S. L. (1995). *Liq. Cryst.*, *18*, 291.

[18] Goodby, J. W. (1999). *Twist grain boundary (TGB) phases in liquid crystals II: Structure and bonding*, Mingos, D. M. P. (Ed.), Springer-Verlag: Berlin, Vol. 95, 83.
[19] Goodby, J. W., Waugh, M. A., Stein, S. M., Chin, E., Pindak, R., & Patel, J. S. (1989). *Nature*, *337*, 449.
[20] Slaney, A. J. & Goodby, J. W. (1991). *J. Mater Chem.*, *1*, 5.
[21] Dhar, R., Srivastava, A. K., & Agrawal, V. K. (2002). *Ind. J. Pure Appl. Phys.*, *40*, 694.
[22] Prasad, S. K., Raja, V. N., Nair, G. G., & Goodby, J. W. (1994). *Mol. Cryst. Liq. Cryst.*, *250*, 239.
[23] Navailles, L., Garland, C. W., & Nguyen, H. T. (1996). *J. Phys. II France*, *6*, 1243.
[24] Werth, M., Nguyen, H. T., Destrade, C., & Isaert, N. (1994). *Liq. Cryst.*, *17*, 863.
[25] Li, M. H., Laux, V., Nguyen, H. T., Sigaud, G., Parois, P., & Isaert, N. (1997). *Liq. Cryst.*, *23*, 389.
[26] Chandrasekhar, S. (1994). *Liquid crystals*, Cambridge University Press: Cambridge, 256.
[27] Petrov, M. & Durand, G. (1996). *J. Phys. France*, *6*, 1259.